

Environmental Research Letters



LETTER

OPEN ACCESS

RECEIVED
25 June 2020

REVISED
25 August 2020

ACCEPTED FOR PUBLICATION
29 September 2020

PUBLISHED
24 November 2020

Original Content from
this work may be used
under the terms of the
[Creative Commons
Attribution 4.0 licence](#).

Any further distribution
of this work must
maintain attribution to
the author(s) and the title
of the work, journal
citation and DOI.



Socio-economic disparities in exposure to urban restaurant emissions are larger than for traffic

R U Shah^{1,2,3} , E S Robinson^{1,2,4} , P Gu^{1,2,5} , J S Apte^{6,7,8} , J D Marshall⁹ , A L Robinson^{1,2} and A A Presto^{1,2}

¹ Center for Atmospheric Particle Studies, Carnegie Mellon University, Pittsburgh, PA 15213, United States of America

² Mechanical Engineering, Carnegie Mellon University, Pittsburgh, PA 15213, United States of America

³ Now at: Environmental Defense Fund, San Francisco, CA 94105, United States of America

⁴ Now at: Department of Environmental Health and Engineering, Johns Hopkins University, Baltimore, MD 21218, United States of America

⁵ Now at: California Air Resources Board, Sacramento, CA 95814, United States of America

⁶ Department of Civil and Environmental Engineering, University of California, Berkeley, Berkeley, CA 94720, United States of America

⁷ School of Public Health, University of California, Berkeley, Berkeley, CA 94720, United States of America

⁸ Formerly at: Department of Civil, Architectural and Environmental Engineering, The University of Texas at Austin, Austin, TX 78712, United States of America

⁹ Department of Civil and Environmental Engineering, University of Washington, Seattle, WA 98195, United States of America

E-mail: apresto@andrew.cmu.edu

Keywords: particulate matter, urban air pollution, restaurant emissions, environmental justice, health and exposure

Supplementary material for this article is available [online](#)

Abstract

Restaurants and vehicles are important urban sources of particulate matter (PM). Due to the ubiquitous presence of these sources within cities, large variabilities in PM concentrations occur in source-rich environments (e.g. downtown), especially during times of peak activity such as meal times and rush hour. Due to intracity variations in factors such as racial-ethnic composition and economic status, we hypothesized that certain socio-economic groups living closer to sources are exposed to higher PM concentrations. To test this hypothesis, we coupled mobile PM measurements with census data in two midsize US cities: Oakland, CA, and Pittsburgh, PA. A novel aspect of our study is that our measurements are performed at a high (block-level) spatial resolution, which enables us to assess the direct relationship between PM concentrations and socio-economic metrics across different neighborhoods of these two cities. We find that restaurants cause long-term average PM enhancements of 0.1 to 0.3 $\mu\text{g m}^{-3}$ over length scales between 50 and 450 m. We also find that this PM pollution from restaurants is unevenly distributed amongst different socio-economic groups. On average, areas near restaurant emissions have about 1.5 \times people of color (African American, Hispanic, Asian, etc), 2.5 \times poverty, and 0.8 \times household income, compared to areas far from restaurant emissions. Our findings imply that there are socio-economic disparities in long-term exposure to PM emissions from restaurants. Further, these socio-economic groups also frequently experience acutely high levels of cooking PM (tens to hundreds of $\mu\text{g m}^{-3}$ in mass concentrations) and co-emitted pollutants. While there are large variations in socio-economic metrics with respect to restaurant proximity, we find that these metrics are spatially invariant with respect to highway proximity. Thus, any socio-economic disparities in exposure to highway emissions are, at most, mild, and certainly small compared to disparities in exposure to restaurant emissions.

1. Introduction

Exposure to urban fine particulate matter (PM_{2.5}) is a serious global health risk [1–3]. Intra-urban variability in PM_{2.5} concentrations is strongly influenced by spatial and temporal patterns of anthropogenic

sources; two important urban sources are commercial cooking and vehicular traffic. Cooking PM is higher in locations and during times of commercial cooking activities (i.e. near restaurants and during meal preparation times), and vehicular PM is higher on or near highways, especially during periods of peak

activity of heavy-duty diesel trucks. Real-time measurements of spatial variabilities in PM composition in the past decade have shown large intra-urban spatial gradients in the impacts of these sources [4–13].

The long-term averages of $\text{PM}_{2.5}$ are higher ($0.5\text{--}2\ \mu\text{g m}^{-3}$) in affected neighborhoods (e.g. city centers a.k.a. ‘downtowns’, neighborhoods with high restaurant density, etc), compared to concentrations reported by stationary reference monitors at urban background sites [14, 15], implying higher long-term exposures for residents of such source-rich neighborhoods. These residents are also frequently exposed to short-lived, high concentrations of these pollutants, which also has health concerns [16]. For example, Robinson *et al* [10], showed that individual restaurant plumes result in intermittent, significantly enhanced cooking PM concentrations (tens to hundreds of $\mu\text{g m}^{-3}$) at the neighborhood scale ($\sim 400\text{ m}$). Further, near points of emission, these plumes are rich in ‘ultrafine’ particles (diameter $<100\text{ nm}$) [8, 17–19], which is a serious concern because health risk from inhalation of particulate matter may increase with decreasing particle size [20–22]. It is thus evident that over the course of a typical day, people living in certain urban neighborhoods can have higher long-term and acute exposures to $\text{PM}_{2.5}$.

Socio-economic factors such as household income, poverty, and racial-ethnic distribution can vary across neighborhoods within a city [23, 24], and also on an inter-city basis [25]. Large variabilities in pollutant levels and exposures across such neighborhoods can then also result in disparities in pollution exposure for certain socio-economic groups [26]. A recent study by Tessum *et al* [27], estimated that emissions along the supply-chain of goods and services exert unequal PM exposures among the US’s diverse racial-ethnic groups, with African American and Hispanic groups bearing a 60% excess pollution burden. While this finding offers a crucial insight into the socio-economic disparity in exposure to PM at a national scale, it does not provide an explicit link between specific urban PM sources and socio-economic disparities in near-source exposure. Several other environmental justice studies have explored this direct link using either dispersion modeling of pollutants across an area, and/or a network of stationary monitors with geospatial interpolation (e.g. Kriging) and regression (e.g. land use regression) [28–37]. In contrast, high-spatial-resolution measurements of pollutant concentrations have been rarely coupled with socio-economic information [19].

Our novel approach in this study is to couple socio-economic information with mobile measurements of source-resolved PM components (e.g. from cooking) conducted at block-level spatial resolution. The objective of this study is three-fold. First, we assess the spatial extents of cooking PM enhancements in the immediate ($\sim 500\text{ m}$) vicinity of restaurants. To achieve this objective, we use

previously published datasets generated from mobile aerosol mass spectrometry measurements in two midsize US cities: Oakland, CA and Pittsburgh, PA [7, 9]. These measurements were performed over multiple weeks, thereby providing robust spatial and temporal patterns of these pollutants at block-level spatial resolution.

Our second objective is to investigate socio-economic disparities in exposure to these cooking PM enhancements. Data provided by the US Census at the block group level provides information such as racial-ethnic composition and household income at block-level spatial resolution. We couple our assessments from the first objective to this census information about Oakland and Pittsburgh, to calculate the average socio-economic composition of the population groups that are exposed to high long-term and acute levels of cooking PM.

Lastly, recent studies have shown that contributions of urban carbonaceous PM from vehicles and restaurants are comparable [7, 9, 38]. However, since these two sources are not always spatially correlated (e.g. see figure 1, and Robinson *et al* [11].), our third objective is to contrast these two sources in terms of socio-economic disparities in exposure to their emissions. Analogous to the first two objectives, we characterize concentrations of fuel-combustion PM, and socio-economic factors, with respect to highway proximity.

2. Methods

2.1. Mobile sampling

As part of the Center for Air, Climate, and Energy Solutions (CACES, www.caces.us) project, we carried out mobile sampling studies in two cities: Pittsburgh, PA and Oakland, CA. Pittsburgh measurements occurred between August 2016 and February 2017. Oakland measurements occurred largely in July 2017. Due to repeated daily sampling during these periods, we sampled nearly all street blocks in downtown and some urban residential neighborhoods on at least 12 different days. Measurements in Oakland were typically between 8 AM and 5 PM local time, while those in Pittsburgh were typically between 8 AM and 8 PM local time.

We deployed the same mobile laboratory and instrumentation suite in both these locations. The key instruments were: a) a high-resolution time-of-flight aerosol mass spectrometer (HR-ToF-AMS, hereafter ‘AMS’; Aerodyne Research Inc [39].) to measure mass concentrations of non-refractory sub-micron particles (PM_1), and b) a seven-wavelength, dual-spot aethalometer (AE33, Magee Scientific) to measure mass concentrations of refractory black carbon (BC; typically emitted from heavy-duty diesel-combustion trucks). Detailed descriptions of the sampling platform design and quality assurance methods can be found in Shah *et al* [9]. and

Gu *et al* [7]. A map of all AMS data in Pittsburgh and Oakland are shown in figures 1 and S1 (<https://stacks.iop.org/ERL/15/114039/mmedia>), respectively.

2.2. Data analysis

2.2.1. Source-apportionment of PM

We processed AMS data using SQUIRREL 1.57I and PIKA 1.16I routines [40] in Igor Pro 6.37 (Wavemetrics, Lake Oswego, OR;). The average total measured PM₁ was 11.3 and 10.2 $\mu\text{g m}^{-3}$ in Oakland and Pittsburgh, respectively, with the carbonaceous contribution exhibiting the largest spatial and temporal variability (2–3 $\mu\text{g m}^{-3}$) in both cities. Using chemical source-apportionment analysis of the organic PM in both cities' datasets, we identified a cooking-related factor (average 14% and 9% contribution to average total PM₁ in Oakland and Pittsburgh, respectively) and a traffic-related factor (average 9% and 7% contribution to average total PM₁ in Oakland and Pittsburgh, respectively). Cooking PM emissions are almost entirely composed of organic matter [41], so this cooking factor represents the entire contribution of cooking sources to PM. Vehicular PM emissions are a mixture of organic matter and black carbon, and thus the sum of these two components represents the total contribution of vehicles to PM. We based the source-apportionment on the following: (a) the chemical mass spectra of the PM components are consistent with previously published mass spectra of cooking and vehicle exhaust measurements; (b) the diurnal profiles of these PM components resemble the expected pattern of the corresponding activity e.g. cooking PM peaks during typical times of peak restaurant activity. Details of source-apportionment methods and quality assurance are described in previous companion papers [7, 9]. Further description of the robustness of our source apportionment analyses is provided in the SI. Note that when referring to these source-resolved PM components, we only refer to the primary emissions i.e. those directly emitted in the form of PM, and not any additional secondary PM that may form as these plumes undergo atmospheric physical/chemical processes [42].

2.2.2. Near-source spatial extent estimations

We performed all geospatial analyses in Q-GIS open-source software. We downloaded locations of restaurants and food trucks (hereafter collectively referred to as restaurants) from multiple sources: local health department websites [43–45], and scraping the Yelp.com [46] website application programming interface [11]. We obtained geographic shapefiles of highways from the public data repositories of Alameda [47] and Allegheny [48] counties (for Oakland and Pittsburgh, respectively). For all mobile sampling locations, we calculated Euclidean

distances to nearest restaurant and nearest highway point. We then used these distances for binning the measurements as functions of proximity to restaurants, and separately, to highways.

While our measurements have a nominal 100 m spatial resolution on latitudinal and longitudinal dimensions, projecting them on to a 'distance-from-source' dimension increases their resolution even more, because of multiple, non-uniformly distributed sources (e.g. restaurants) in the city. We thus arbitrarily used a 30 m lengthscale to resolve our measurements on this dimension.

We classified our pollutant measurements into 30 m 'distance-from-source' bins (where 'pollutant' is a source-resolved PM component, and 'source' is restaurants or highways). Within each 30 m bin, we calculated the median pollutant concentration. There were typically $10^2 - 10^3$ samples in bins within 400 m of source, as shown in figure S4. In the interest of comparing near-source enhancements, we normalized these median concentrations to the median in the farthest distance bin with at least 50 samples. Following Apte *et al* [6], we fit these medians using an exponential model to characterize the pollutant's fall-off behavior with increasing distance from their sources (restaurants for cooking PM, highways for traffic-related PM):

$$f(d) = \alpha + \beta \cdot \exp(-d/k), \quad (1)$$

where α is the median concentration in the farthest distance bin (nominally this should be unity, since we are normalizing near-source medians to this concentration; however, we did not pin α), β is the fractional enhancement immediately next to the source i.e. at $d=0$ (e.g. $\beta = 0.5$, i.e. $\alpha + \beta = 1.5$, implies that immediately next to restaurants, median cooking PM is $1.5 \times$ background), and k is the characteristic e-folding lengthscale describing how fast, with increasing distance (d) from source, the pollutant concentration decays to background level. Co-efficients α , β , and k are determined by the iterative Levenberg-Marquardt non-linear least-squares algorithm in Igor Pro.

Due to wind recirculation and turbulence between buildings, resolving measurements based on wind direction can be challenging. Hence, we did not classify our measurements into 'upwind' and 'downwind' of source. The fall-off behavior characterized by equation (1) should thus be considered an average representation of a uniform buffer of radius d around the source.

2.2.3. Socio-economic analyses

We downloaded socio-economic data from the US Census Bureau's 2017 community surveys, resolved at the block level [49]: racial-ethnic composition

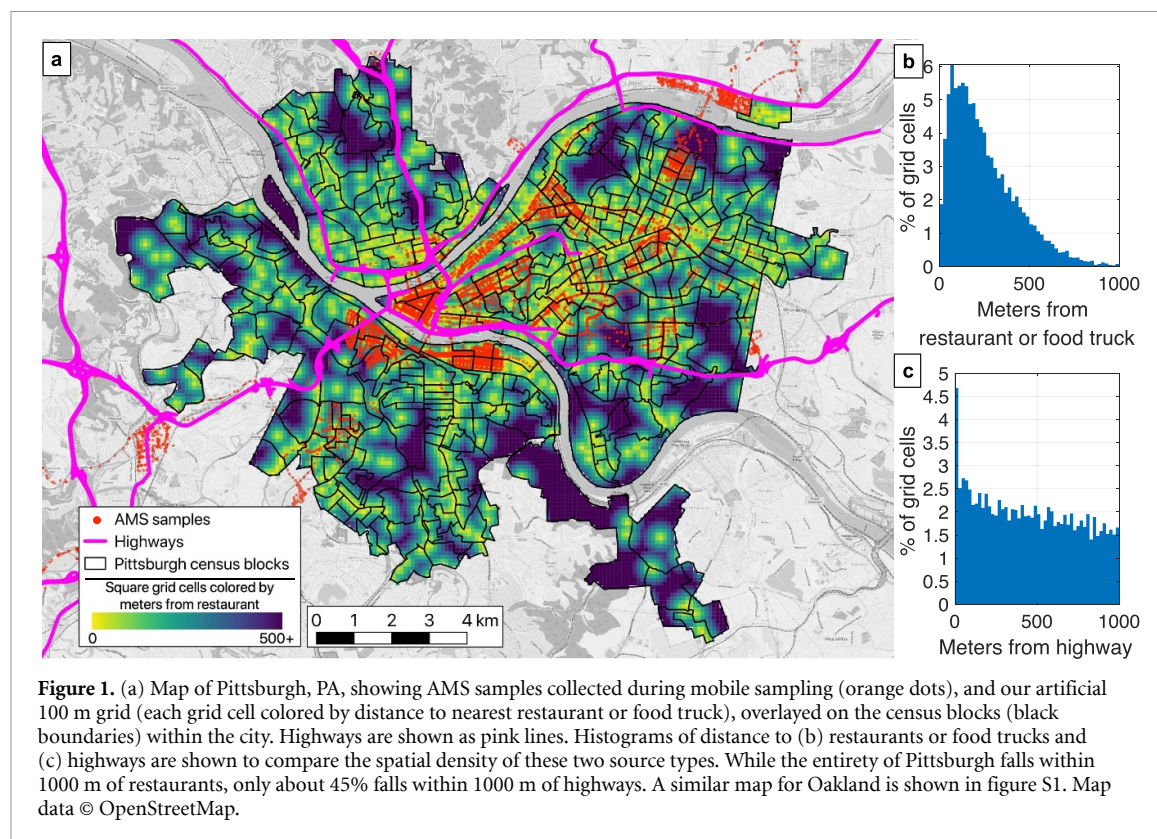


(table B03002¹⁰), median household income (table B19013), and poverty (table B17017; poverty is defined as the number of households with income below a certain threshold). Figure 1(a) shows these census blocks. Clearly, with our mobile sampling, we oversampled some census blocks, while under-sampling (or not sampling at all) other census blocks. Coupling socio-economic metrics directly to our sampling locations would have propagated these biases and skewed our results towards oversampled blocks. To avoid this, we overlaid an artificial 100 m grid over the entire city, and used these uniformly-spaced grid cells to represent the census blocks within which they fall.

For each 100 m grid cell, we calculated the Euclidean distance of the grid cell center to the nearest restaurant and highway point in Q-GIS. We then classified the grid cells into 30 m bins of proximity to sources (same as how we classified our measurements into 30 m bins of source-proximity earlier), and calculated the city-wide distributions of these proximities (as shown in figures 1(b) and (c)). We also calculated averages of each socio-economic metric (e.g. median household income) within each of these proximity bins. This effectively results in a weighted average of each socio-economic metric, where each

census block's weight is simply the fraction of total grid cells falling inside it. With increasing distance from restaurants or highways, the number of people of different races and ethnicities can be confounded with other factors such as density of housing, zoning laws in certain census blocks, etc. For example, figure S6 shows that population has a decreasing trend with increasing distance from restaurants. Hence, to control for these confounding factors, we used the fractional contribution of these population groups instead of absolute population.

Lastly, we used our e-folding lengthscale calculated from equation (1) to broadly classify the binned averages of socio-economic metrics as either 'near' or 'far from' restaurants. In other words, if $k = 200$ m, then the averages of socio-economic metrics in bins less than 200 m are further averaged to represent a 'near restaurants' average, while the other bins (>200 m) are further averaged to represent a 'far from restaurant' average.

3. Results and discussion

3.1. Spatial influence of particulate matter (PM) emissions from restaurants

Figure 2 shows the fall-off behavior of cooking PM with increasing distance from restaurants in Oakland and Pittsburgh. Data are presented as binned median enhancements of cooking PM relative to background, fitted by the three-parameter exponential model (equation (1)) to characterize the e-folding lengthscale, k . We limit the abscissae to 400 m because

¹⁰ People of all races who are Hispanic or Latino shall be referred to as Hispanic in this study. Our analyses for White, African American, Asian, and Other groups use data on people that are not of Hispanic origin (listed as 'not Hispanic: White', 'not Hispanic: African American', etc in census table B03002).

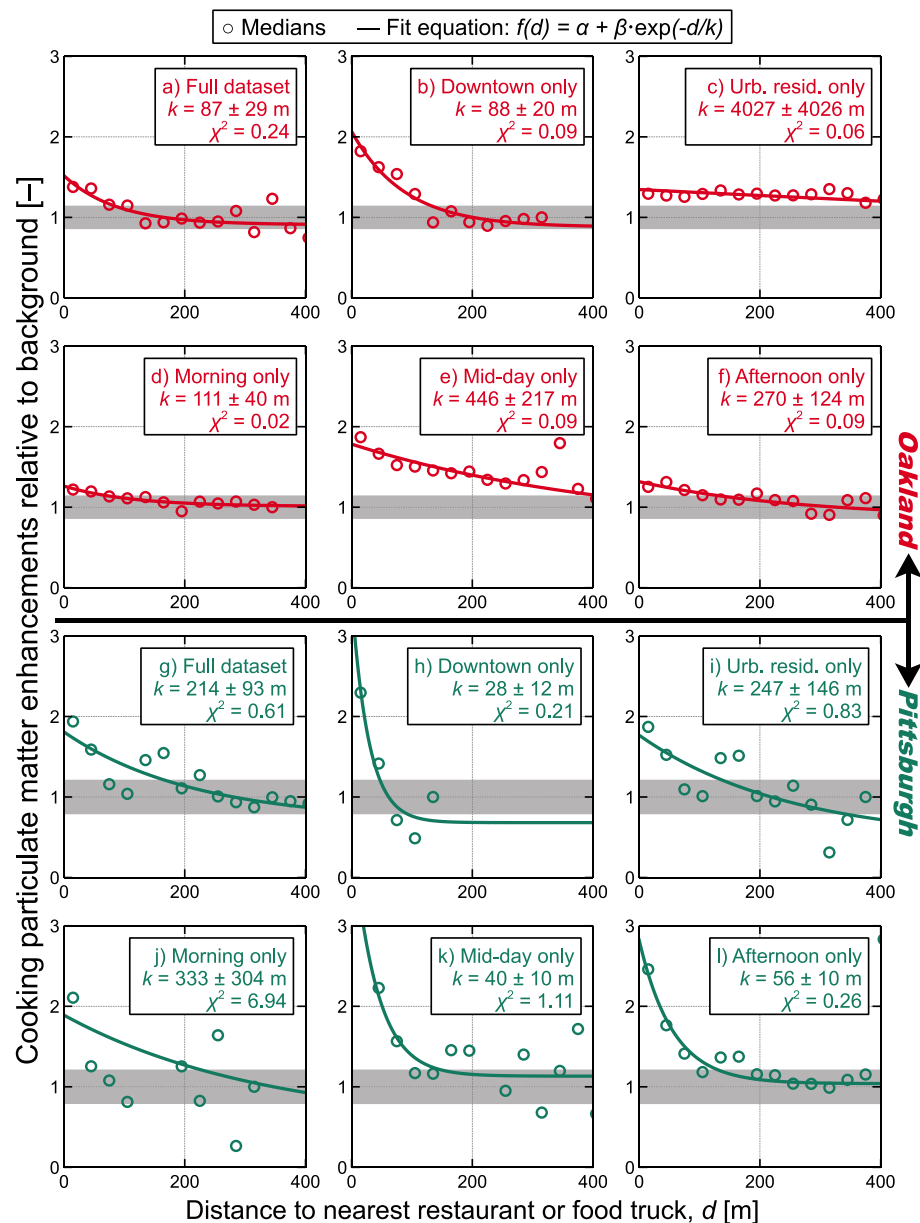


Figure 2. Fall-off behavior of cooking particulate matter with increasing distance from restaurants in Oakland (panels a–f) and Pittsburgh (panels g–l). Since data are presented as enhancements relative to background levels, the fits describe the decay of median relative cooking PM enhancements from immediately next to sources (β) to background level (α), and the spatial extent (k) around restaurants where these enhanced levels are observed. The shaded gray regions are uncertainties in background cooking PM; specifically, 1σ of median concentrations measured >500 m from restaurants ($\pm 15\%$ in Oakland, $\pm 20\%$ in Pittsburgh). Standard deviations of k are calculated during fitting. χ^2 is the squared residual of fit. ‘Urb. resid.’ = urban residential. While the afternoon panel in Oakland (panel (f)) only includes data till 5 PM local time, that for Pittsburgh (panel (l)) includes dinner time data i.e. till 8 PM local time.

we have little to no sampling coverage beyond this point in both Oakland and Pittsburgh (as shown in figure S4).

Figure 2 shows data and fits for the entire datasets in both cities (panels a and g), as well as for data stratified by land-use areas (downtown and urban residential portions of both cities are analyzed separately in panels (b), (c), (h), and (i)), and by different periods of restaurant activity (morning, mid-day, and afternoon, in panels (d)–(f), and (j)–(l)). A map of downtown and urban residential neighborhoods of Oakland and Pittsburgh is shown in figure S2. For each

panel of figure 2, bins with fewer than 20 measurements are considered insufficiently sampled, and are thus neither graphed nor included in fitting. We set this tolerance following the findings of Apte *et al* [6], and Messier *et al* [50]. Lack of data in the downtown panels ((b) and (h)) is due to high restaurant density in these relatively small neighborhoods, resulting in most measurements falling within a few hundred meters of the nearest restaurant, and virtually no measurements beyond that point.

In both cities’ datasets, the exponential model generates a wide range of k -values for different

spatial and temporal strata. This variability seems to be affected by both restaurant cooking activity (e.g. higher emissions during mid-day), as well as restaurant density. As mentioned earlier, some of this variability is likely also due to meteorological factors (e.g. local wind speed and direction), which we did not account for. Hence, for the subsequent socio-economic disparity analyses in Oakland, we will use a central k of 270 m, and will use the 87 m and 442 m as lower and upper bounds for testing sensitivity. Similarly, in Pittsburgh, we will use a central k of 214 m, with 40 m and 333 m as lower and upper bounds.

In the full Oakland dataset, relative enhancements in cooking PM immediately next to restaurants (i.e. at $d = 0$) are $1.5\times$ background levels (panel (a)). With increasing distance, PM decays to background levels with an e-folding lengthscale, k , of 87 m. Downtown Oakland has a similar k -value, albeit with a higher local enhancement, β , of $2\times$ background, while cooking PM in urban residential Oakland is almost spatially invariant. This is likely because of the very low restaurant density in this part of Oakland (12 km^{-2}). As a result, it may be challenging to distinguish emissions from restaurants versus that from household kitchens. In other words, all kitchens (restaurants and households) may collectively act as an area source, raising the overall background cooking PM level of the neighborhood, but without any discernible point sources. This is consistent with the findings in Shah *et al* [9]: cooking PM in urban residential Oakland was shown to have very little spatial and temporal variability. Because of this invariance with respect to restaurant proximity, the k -value generated by the exponential model ($\sim 4\text{ km}$) is not physically meaningful. In contrast, downtown Oakland, with a higher restaurant density of 56 km^{-2} , exhibits a clear exponential fall-off of cooking PM with increasing distance from restaurants.

Stratifying the data by diurnal periods also offers meaningful insights. In Oakland, the morning (8 am to 11 am) and afternoon (2 pm to 5 pm) periods have low β of $1.2\times$ and $1.3\times$ background, indicating low commercial cooking activity during these periods. Conversely, the mid-day period (11 am to 2 pm) has a higher β value of $1.8\times$ background, showing the effect of increased cooking emissions. Further, a k of 442 m during this period indicates a farther extent of restaurant influence on nearby air quality. Both mid-day and afternoon periods in Pittsburgh have high β of $4\times$ (off-scale in figure 2(k)) and $2.7\times$ background, indicating high commercial cooking activity in these periods. As mentioned earlier, unlike in Oakland, we performed measurements in Pittsburgh after 5 PM local time. Hence, while the afternoon panel in Oakland (panel (f)) shows little influence of restaurants, the same for Pittsburgh (panel (l)) shows a clear dinner-time effect.

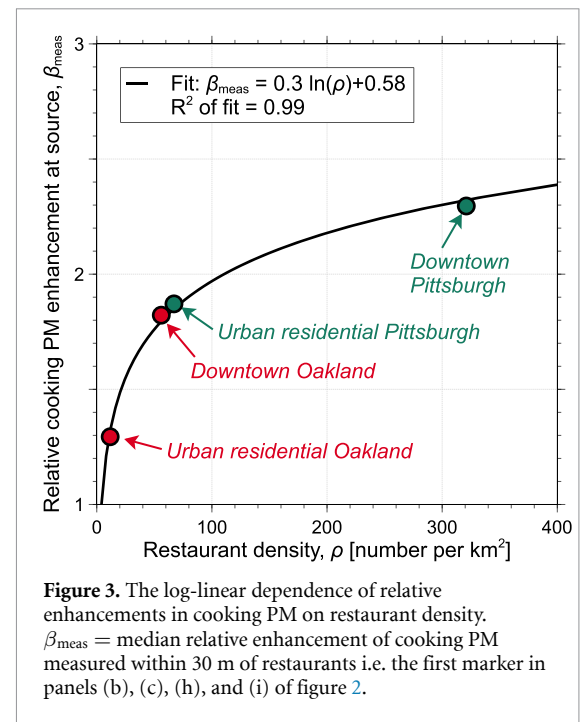


Figure 3. The log-linear dependence of relative enhancements in cooking PM on restaurant density. β_{meas} = median relative enhancement of cooking PM measured within 30 m of restaurants i.e. the first marker in panels (b), (c), (h), and (i) of figure 2.

Overall, the quality of fits (χ^2) is lower in Pittsburgh than in Oakland. This is because absolute cooking PM concentrations are lower in Pittsburgh (as shown in figures 4 and S4). As a result, normalizing to background levels amplified the noise in the Pittsburgh panels of figure 2 (especially in the morning, when restaurant emissions are lowest). Despite this, the dependence of cooking PM on restaurant proximity is still reasonably well constrained by the exponential model (as indicated by the χ^2 of fits). In the full Pittsburgh dataset (panel (g)), enhancements immediately next to restaurants are $1.8\times$ background levels. With increasing distance, cooking PM decays with an e-folding lengthscale, k , of 214 m. Downtown and urban residential neighborhoods of Pittsburgh also have higher β ($3\times$ and $1.8\times$ background) compared to respective neighborhoods of Oakland. Pittsburgh has a higher restaurant density than Oakland, which explains why it has a higher β than Oakland (panel (a)). This is another example of the effect of restaurant density: downtown and urban residential Pittsburgh have restaurant densities of 321 km^{-2} and 67 km^{-2} , respectively (much higher than the 56 km^{-2} and 12 km^{-2} in respective parts of Oakland). Due to this, urban residential Pittsburgh still exhibits a discernible, albeit noisy dependence on restaurant proximity (unlike urban residential Oakland). The e-folding lengthscale, k , in urban residential Pittsburgh (247 m) is similar to that for the entire dataset (214 m).

As discussed above, relative enhancements of cooking PM near restaurants are not only affected by proximity and activity, but also by density of restaurants. Figure 3 shows this dependence more clearly. In different land-use areas of Oakland and

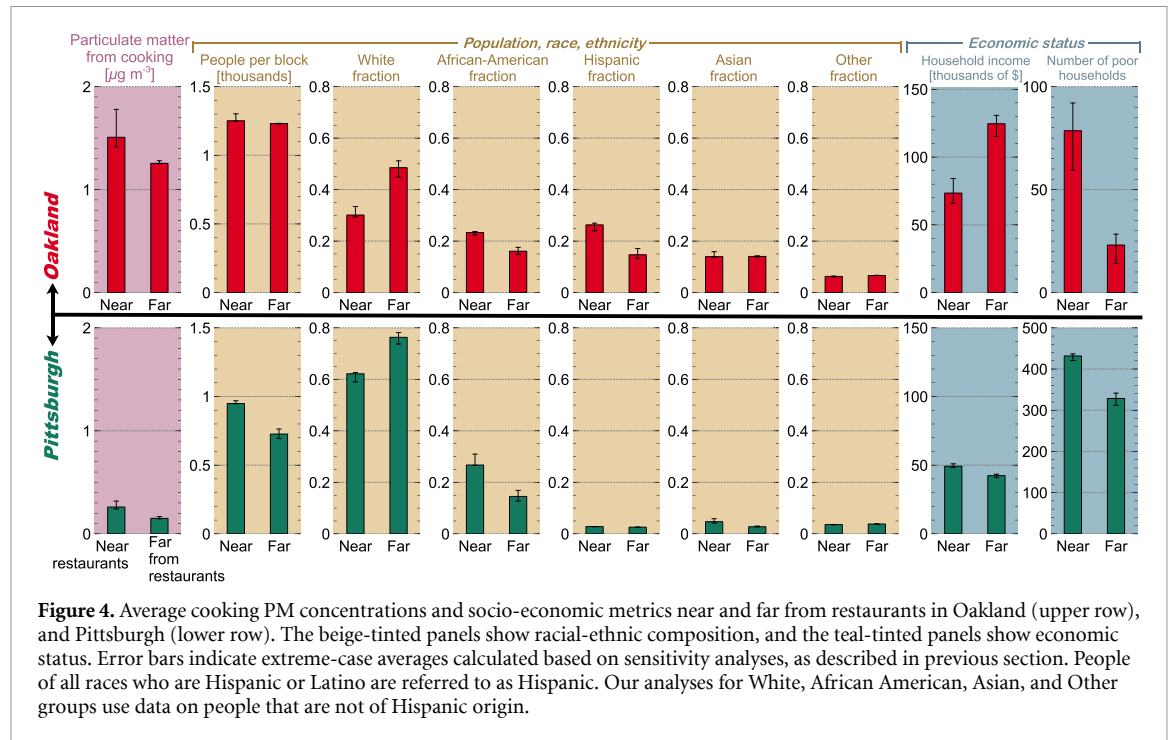


Figure 4. Average cooking PM concentrations and socio-economic metrics near and far from restaurants in Oakland (upper row), and Pittsburgh (lower row). The beige-tinted panels show racial-ethnic composition, and the teal-tinted panels show economic status. Error bars indicate extreme-case averages calculated based on sensitivity analyses, as described in previous section. People of all races who are Hispanic or Latino are referred to as Hispanic. Our analyses for White, African American, Asian, and Other groups use data on people that are not of Hispanic origin.

Pittsburgh, the measured enhancement within 30 m of restaurants, β_{meas} (i.e. the first marker in panels (b), (c), (h), and (i) of figure 2), exhibits a log-linear dependence on restaurant density. It is worth noting that in addition to restaurant count, restaurant density was also a cooking PM predictor variable identified by the land-use regression model of Robinson *et al* [11] in Oakland.

3.2. Socio-economic disparities in exposure to restaurant emissions

In this section, we couple spatial influence of particulate matter emissions from restaurants with socio-economic metrics around restaurants. As described earlier, we first binned socio-economic metrics (e.g. household income) in the same 30 m bins of restaurant proximity as used in figures 1 and 2. This preliminary binning is shown for Pittsburgh and Oakland in figure S6. Clearly, in both cities, certain socio-economic patterns exist with respect to restaurant proximity. For instance, in both cities, poverty decreases with increasing distance from restaurants. The fraction of African American population also decreases, while fraction of White population increases with increasing distance from restaurants.

To characterize these socio-economic metrics with respect to restaurant PM emissions, we use the e-folding lengthscale (k) calculated in the previous section as the spatial extents of influence of particulate matter emissions from restaurants. We use this lengthscale to broadly classify the cities into two regions: near restaurants (i.e. distance to nearest restaurant $< k$), and far from restaurants (distance to nearest restaurant $> k$). Because this delineation is

sensitive to k , we also use the lower and upper bounds of k observed in the previous section as our extreme cases to test sensitivity. These values, with sensitivity estimates, are shown in figure 4.

As shown in figure 4, average cooking PM concentrations near restaurants are 0.1 to 0.3 $\mu\text{g m}^{-3}$ higher than those far from restaurants. While these differences may seem small, two points should be noted: first, while these represent long-term and city-wide averages, certain areas (e.g. downtown, areas with high restaurant density) have long-term average cooking PM enhancements as large as 1 $\mu\text{g m}^{-3}$ (especially during peak restaurant activity periods), as shown in figures 2 and 3. Second, as discussed in the next section, these differences also represent large variations in acute cooking PM levels, which are dampened by the multiple stages of aggregation performed on >15000 individual measurements in each city.

Comparing Oakland and Pittsburgh in figure 4 reveals intercity disparities in cooking PM concentrations and racial-ethnic composition. Oakland has 4 \times higher average cooking PM concentration than Pittsburgh. Oakland also has 1.5 \times more people per census block than Pittsburgh, with 4 \times higher Hispanic fraction, 3 \times higher Asian fraction, and 0.7 \times lower White fraction than Pittsburgh. The overall economic status in Oakland is higher than that in Pittsburgh (i.e. higher household income, lower poverty). This is likely a result of other factors, such as dominant industry type, that influence the overall standard of living.

Figure 4 also shows intracity socio-economic disparities in both cities. Overall, near restaurant

emissions, the total fraction of people of color¹¹ is higher, White fraction is lower, poverty is higher, and median household income is lower compared to far from restaurant emissions. In Oakland, African-American and Hispanic fractions living near restaurant emissions are respectively $1.5\times$ and $1.8\times$ higher, while White fraction is $0.6\times$ lower, compared to far from restaurant emissions. Similarly, near Pittsburgh's restaurant emissions, the African-American fraction is $1.8\times$ higher, while White fraction is $0.8\times$ lower, compared to far from restaurant emissions.

Oakland's median household income near restaurant emissions is $0.6\times$ lower, while poverty (= number of households with income below poverty line) is $3.4\times$ higher than far from restaurants. While Pittsburgh's median household income near restaurant emissions is slightly higher ($1.1\times$) than far from restaurants, poverty is still $1.3\times$ higher near restaurants than far from restaurants. That income and poverty are anti-correlated in Oakland, but not so in Pittsburgh, may due to other differences between the two cities, as proposed above. For example, Oakland is part of the San Francisco-Oakland-San Jose combined statistical area, and thus has diffusion of population across these neighboring city limits. On the other hand, Pittsburgh is the only major city in the greater Pittsburgh metropolitan area, with a major industrial area on the outskirts, which likely plays a role in the lower median household income far from restaurants.

While cooking PM concentrations are unevenly distributed for certain socio-economic groups, they are also evenly distributed for other groups. For example, in Oakland, fractions of Asian and Other groups are similar (within 10%) near and far from restaurants emissions. Similarly, Pittsburgh's Hispanic and Other groups are similar (within 10%) near and far from restaurants.

As noted above, the error bars in figure 4 represent sensitivity of the results to the choice of k used for classifying areas as near or far from restaurants. Using the lower and upper bounds of k identified in figure 2 changes the specific concentrations and socio-economic metrics, but it does not change the overall conclusions. Cooking PM concentrations are higher near restaurants, where there are more people of color, and economic status is lower, compared to far from restaurants.

In summary, the results presented in figure 4 show that there are intercity and intracity differences in cooking PM concentrations and socio-economic metrics in Oakland and Pittsburgh. That poverty and total fraction of people of color is higher near restaurants strongly implies that these socio-economic groups are exposed to higher cooking PM concentrations, and thus bear a higher probability of related

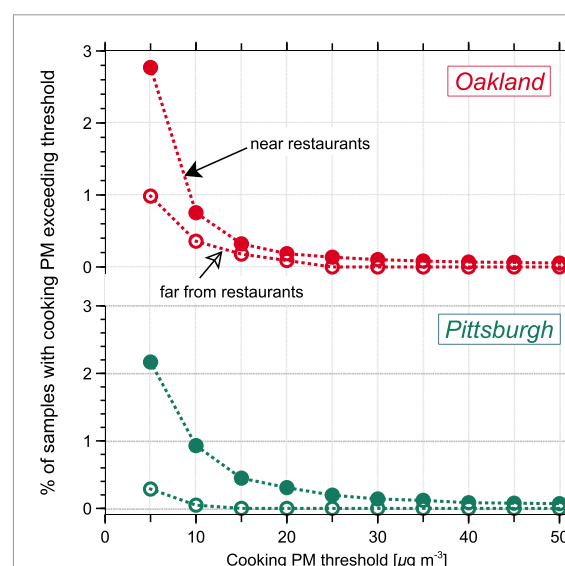


Figure 5. Percentage of samples with cooking PM exceeding different thresholds near and far from restaurants in Oakland and Pittsburgh. The purpose of this visualization is to emphasize the importance of acutely large cooking PM concentrations near restaurants. *Note:* dotted lines between markers are only to guide the eye.

health risks, compared to White and richer population groups.

3.3. Acute cooking PM concentrations due to restaurant emissions

In figure 4, we showed that long-term and city-wide averages of near-restaurant local PM enhancements are $0.1\text{--}0.3 \mu\text{g m}^{-3}$, with certain neighborhoods of high restaurant density having enhancements as large as $1 \mu\text{g m}^{-3}$. While these differences are only 1–2% of typical total urban PM (up to $\sim 10\%$ in high restaurant density areas), these differences represent acutely high cooking PM concentrations, which are obscured when aggregated at multiple stages. To explore this information, we now revisit the raw measurements i.e. prior to any aggregation. Figure 5 shows the percentage of total samples near and far from restaurants with cooking PM concentration exceeding a series of thresholds. These threshold crossings can be thought of as cooking emission plumes of various intensities, and how often one experiences these acute levels. For instance, figure 5 shows that in Oakland and Pittsburgh, acute exposures to $>5 \mu\text{g m}^{-3}$ cooking PM are respectively $3\times$ and $7\times$ more frequent near restaurants, compared to those far from restaurants.

While the data in figure 5 show cooking PM concentrations exceeding thresholds of $5\text{--}50 \mu\text{g m}^{-3}$, concentrations as high as $200 \mu\text{g m}^{-3}$ have previously been observed within 200 m downwind distance of restaurants [10]. It is thus evident that the socio-economic groups living near restaurant emissions experience not only the additional $0.1\text{--}0.3 \mu\text{g m}^{-3}$ of long-term cooking PM concentrations, but also frequently experience these acute concentrations. Further, as mentioned earlier, exposure to these

¹¹ We use the term 'people of color' to refer to African American, Asian, Hispanic and Other (Hawaiian, American Indian, Alaskan, Pacific Islander).

plumes does not just increase exposure to mass concentrations of particulate matter, but also to the ultrafine particle number concentrations [8, 51, 52], which may have more serious health effects [21]. Lastly, other pollutants co-emitted with PM from cooking activities (e.g. carcinogenic aldehydes emitted from frying [53, 54]) also increase the health risks associated with these acute exposures near restaurants.

3.4. Socio-economic disparities in exposure to traffic emissions

As mentioned earlier, we resolved our observed PM into two vehicular components: an organic component (chemically referred to in literature as 'hydrocarbon-like organic aerosol' or HOA), and a refractory component (black carbon or BC). Summing these two components provides an estimate of total vehicular PM. We analyzed these vehicular PM concentrations with respect to highway proximity, analogous to cooking PM and restaurant proximity. Overall, we find no socio-economic disparities with respect to vehicular PM emissions near highways in Oakland and Pittsburgh. We briefly discuss these findings below, with details in the SI.

Figure S7 shows that with increasing distance from source, the fall-off lengthscales of vehicular PM are much smaller (<55 m) compared to cooking PM. While our findings are consistent with previous measurements, fall-off lengthscales as high as 420 m have also been reported in other studies [6, 55]. This is not surprising, because as we showed with our cooking PM analyses in figure 2, the lengthscale k can be sensitive to factors such as restaurant density and peak cooking periods. Analogous to that, these variances in highway-influence lengthscales could likely be explained by intuitive factors such as traffic volume, vehicle fleet (e.g. age and fuel), and season [56, 57]. Our findings are thus consistent with literature in that depending on these influencing factors, highways can influence PM levels within a 40 to 400 m buffer.

Figure S8 shows Oakland's and Pittsburgh's socio-economic patterns with respect to highway proximity. Contrary to patterns with respect to restaurant proximity (figure S6), figure S8 shows that socio-economic factors are spatially invariant with respect to highways. Further, while the majority of the populations of Oakland (67%) and Pittsburgh (90%) live within 500 m of restaurants, a comparatively smaller fraction (36% in Oakland, 25% in Pittsburgh) live within 500 m of highways (figures S1 and 1). Thus, while traffic emissions certainly pose serious health effects to those exposed to them, our analyses show that these exposures are evenly distributed across different socio-economic groups. Lastly,

Robinson *et al* [10]. also showed that acute exposures to restaurant emissions are more frequent than traffic emissions.

4. Conclusions

The novelty of this study is that we coupled high-spatial-resolution measurements of source-resolved particulate matter (PM) to demographic data to investigate environmental justice in PM exposure in two US cities: Oakland, CA, and Pittsburgh, PA. To our knowledge, there are very few studies that have investigated source-resolved PM components at high spatial resolution in other cities [5, 58, 59], all of which were in Europe. Thus, in the absence of more information, we cannot guarantee that other US cities have the same environmental justice patterns as Oakland and Pittsburgh. We address other limitations of our sampling methods and analyses in section S7.

Urban restaurant emissions can influence PM levels at the neighborhood scale. We characterized the spatial extents of this influence using mobile PM measurements. We observe increments in cooking PM levels within a 250 m buffer of restaurants, with variations ranging between approximately 50 and 450 m. These variations arise due to spatial and temporal variables such as restaurant density and peak cooking times. To our knowledge, the work of Robinson *et al* [10]. is the only other study that has explored spatial extents of restaurant plumes, and the range of extents reported in that study are consistent with the findings of this study.

We find that pollution from restaurant emissions is unevenly distributed amongst different socio-economic groups. On average, areas of Oakland and Pittsburgh that are near restaurant emissions have more people of color (i.e. African American, Asian, Hispanic, Hawaiian, American Indian, Alaskan, and Pacific Islander), and also have a lower economic status, compared to areas far from restaurant emissions. This implies that the long-term average cooking PM concentrations breathed by these population groups are $0.1\text{--}0.3\text{ }\mu\text{g m}^{-3}$ higher. In addition to higher long-term exposure, these socio-economic groups also frequently experience acutely high levels of cooking PM (tens to hundreds of $\mu\text{g m}^{-3}$ in mass concentrations, and thousands of ultrafine particle number concentrations [8, 18]), and co-emitted pollutants.


Lastly, we showed that in both Oakland and Pittsburgh, socio-economic factors are invariant with respect to highway proximity. Thus, any socio-economic disparities in long-term and acute exposure to highway emissions are, at most, mild, and certainly small compared to disparities in exposure to restaurant emissions.

Acknowledgments

We thank Dr Zhongju Li and Dr Qing Ye for assistance with measurements in Pittsburgh, and Prof. Peter J Adams for helpful discussions. This work is part of the Center for Air, Climate and Energy Solution (CACES, www.caces.us). This publication was developed under Assistance Agreement No. RD83587301 awarded by the U.S. Environmental Protection Agency. This work has not been formally reviewed by the funding agencies. The views expressed in this document are solely those of the authors and do not necessarily reflect those of the funding agencies. EPA does not endorse any products or commercial services mentioned in this publication. Measurements in Oakland and Pittsburgh were partly funded by Environmental Defense Fund, and National Science Foundation (grant number AGS1543786).


ORCID iDs

R U Shah  <https://orcid.org/0000-0002-4608-1972>

E S Robinson  <https://orcid.org/0000-0003-1695-6392>

P Gu  <https://orcid.org/0000-0003-3519-7942>

J S Apte  <https://orcid.org/0000-0002-2796-3478>

J D Marshall  <https://orcid.org/0000-0003-4087-1209>

A L Robinson  <https://orcid.org/0000-0002-1819-083X>

A A Presto  <https://orcid.org/0000-0002-9156-1094>

References

- [1] Apte J S, Marshall J D, Cohen A J and Brauer M 2015 Addressing global mortality from ambient PM_{2.5} *Environ. Sci. Technol.* **49** 8057–66
- [2] Pope A, Burnett R, Thun M, EE C, D K, I K and GD T 2002 Long-term exposure to fine particulate air pollution JAMA **287** 1132–41
- [3] Dockery D W, Pope C A, Xu X, Spengler J D, Ware J H, Fay M E, Ferris B G and Speizer F E 1993 An association between air pollution and mortality in six US cities *N. Engl. J. Med.* **329** 1753–9
- [4] Mohr C, Richter R, Decarlo P F, Prévôt A S H and Baltensperger U 2011 Spatial variation of chemical composition and sources of submicron aerosol in Zurich during wintertime using mobile aerosol mass spectrometer data *Atmos. Chem. Phys.* **11** 7465–82
- [5] Mohr C, Decarlo P F, Heringa M F, Chirico R, Richter R, Crippa M, Querol X, Baltensperger U and Prévôt A S H 2015 Spatial variation of aerosol chemical composition and organic components identified by positive matrix factorization in the Barcelona region *Environ. Sci. Technol.* **49** 10421–30
- [6] Apte J S, Messier K P, Gani S, Brauer M, Kirchstetter T W, Lunden M M, Marshall J D, Portier C J, Vermeulen R C H and Hamburg S P 2017 High-resolution air pollution mapping with Google street view cars: exploiting big data *Environ. Sci. Technol.* **51** 6999–7008
- [7] Gu P, Li H Z, Ye Q, Robinson E S, Apte J S, Robinson A L and Presto A A 2018 Intracity variability of PM exposure is driven by carbonaceous sources and correlated with land use variables *Environ. Sci. Technol.* **52** [acs.est.8b03833](https://doi.org/10.1021/acs.est.8b03833)
- [8] Ye Q et al 2018 Spatial variability of sources and mixing state of atmospheric particles in a metropolitan area *Environ. Sci. Technol.* **52** 6807–15
- [9] Shah R U, Robinson E S, Gu P, Robinson A, Apte J S and Presto A A 2018 High-spatial-resolution mapping and source apportionment of aerosol composition in Oakland, California using mobile aerosol mass spectrometry *Atmos. Chem. Phys.* **18** 16325–44
- [10] Robinson E S, Gu P, Ye Q, Li H Z, Shah R U, Apte J S, Robinson A L and Presto A A 2018 Restaurant impacts on outdoor air quality: elevated organic aerosol mass from restaurant cooking with neighborhood-scale plume extents *Environ. Sci. Technol.* **52** 9285–94
- [11] Robinson E S, Shah R U, Messier K, Gu P, Li H Z, Apte J S, Robinson A L and Presto A A 2019 Land-use regression modeling of source-resolved fine particulate matter components from mobile sampling *Environ. Sci. Technol.* **53** 8925–37
- [12] Grivas G, Stavroulas I, Liakakou E, Kaskaoutis D G, Bougiatioti A, Paraskevopoulou D, Gerasopoulos E and Mihalopoulos N 2019 Measuring the spatial variability of black carbon in Athens during wintertime *Air Qual Atmos Health* **12** 1405–17
- [13] Caubel J J, Cados T E, Preble C V and Kirchstetter T W 2019 A distributed network of 100 black carbon sensors for 100 days of air quality monitoring in West Oakland, California *Environ. Sci. Technol.* **53** 7564–73
- [14] Chambliss S E et al 2020 Comparison of mobile and fixed-site black carbon measurements for high-resolution urban pollution mapping *Environ. Sci. Technol.* **54** 7848–57
- [15] Li H Z, Gu P, Ye Q, Zimmerman N, Robinson E S, Subramanian R, Apte J S, Robinson A L and Presto A A 2019 Spatially dense air pollutant sampling: Implications of spatial variability on the representativeness of stationary air pollutant monitor *Atmos. Environ.: X* **2** 100012
- [16] Di Q, Dai L, Wang Y, Zanobetti A, Choirat C, Schwartz J D and Dominici F 2017 Association of short-term exposure to air pollution with mortality in older adults *JAMA* **318** 2446
- [17] Canagaratna M R, Onasch T B, Wood E C, Herndon S C, Jayne J T, Cross E S, Miao L, Lye R C, Kolb C E and Worsnop D R 2010 Evolution of vehicle exhaust particles in the atmosphere *J. Air Waste Manage. Assoc.* **60** 1192–203
- [18] Saha P K et al 2019 Quantifying high-resolution spatial variations and local source impacts of urban ultrafine particle concentrations *Sci. Total Environ.* **655** 473–81
- [19] Ye Q, Li H Z, Gu P, Robinson E S, Apte J S, Sullivan R C, Robinson A L, Donahue N M and Presto A A 2020 Moving beyond fine particle mass: high-spatial resolution exposure to source-resolved atmospheric particle number and chemical mixing state *Environ. Health Perspect.* **128** 17009
- [20] Ferin J, Oberdörster G and Penney D P 1992 Pulmonary retention of ultrafine and fine particles in rats *Am. J. Respir. Cell Mol. Biol.* **6** 535–42
- [21] Oberdörster G 2000 Toxicology of ultrafine particles: in vivo studies *Philos. Trans. R. Soc. A* **358** 2719–40
- [22] Stölzel M, Breitner S, Cyrys J, Pitz M, Wölke G, Kreyling W, Heinrich J, Wichmann H E and Peters A 2007 Daily mortality and particulate matter in different size classes in Erfurt, Germany *J. Expo. Sci. Environ. Epidemiol.* **17** 458–67
- [23] Randolph B and Tice A 2017 Relocating disadvantage in five Australian cities: socio-spatial polarisation under neo-liberalism *Urban Pol. Res.* **35** 103–21
- [24] Maloutas T and Nikiforos S S 2019 Segregation trends in Athens: the changing residential distribution of occupational categories during the 2000s *Reg. Stud.* **34** 462–71
- [25] Yu Z, Zhang H, Tao Z and Liang J 2019 Amenities, economic opportunities and patterns of migration at the city level in China *Asian Pac. Migr. J.* **28** 3–27
- [26] Fujita E M, Campbell D E, Patrick Arnott W, Lau V and Martien P T 2013 Spatial variations of particulate matter and

- air toxics in communities adjacent to the Port of Oakland *J. Air Waste Manage. Assoc.* **63** 1399–1411
- [27] Tessum C W *et al* 2019 Inequity in consumption widens racial-ethnic disparities in air pollution exposure *Proc. Natl Acad. Sci. USA* **116** 6001–6
- [28] Grineski S, Bolin B and Boone C 2007 Criteria air pollution and marginalized populations: environmental inequity in metropolitan Phoenix, Arizona *Soc. Sci. Q.* **88** 535–54
- [29] Germani A R, Morone P and Testa G 2014 Environmental justice and air pollution: a case study on Italian provinces *Ecol. Econ.* **106** 69–82
- [30] Marshall J D, Granvold P W, Hoats A S, McKone T E, Deakin E and W Nazaroff W 2006 Inhalation intake of ambient air pollution in California's South Coast Air Basin *Atmos. Environ.* **40** 4381–92
- [31] Marshall J D 2008 Environmental inequality: Air pollution exposures in California's South Coast Air Basin *Atmos. Environ.* **42** 5499–503
- [32] McLeod H, Langford I H, Jones A P, Stedman J R, Day R J, Lorenzoni I and Bateman I J 2000 The relationship between socio-economic indicators and air pollution in England and Wales: implications for environmental justice *Reg. Environ. Change* **1** 78–85
- [33] Morello-Frosch R, Pastor M and Sadd J 2001 Environmental justice and southern California's "riskycape" The distribution of air toxics exposures and health risks among diverse communities *Urban Affairs Rev.* **36** 551–78
- [34] Pearce J, Kingham S and Zawar-Reza P 2006 Every breath you take? Environmental justice and air pollution in Christchurch, New Zealand *Environ. Plan. A* **38** 919–38
- [35] Samet J M 2001 Urban air pollution and health inequities: a workshop report *Environ. Health Perspect.* **109** 357–74
- [36] Su J G, Larson T, Gould T, Cohen M and Buzzelli M 2010 Transboundary air pollution and environmental justice: Vancouver and Seattle compared *GeoJournal* **75** 595–608
- [37] Giani P, Anav A, De Marco A, Zhaozhong F and Crippa P 2020 Exploring sources of uncertainty in premature mortality estimates from fine particulate matter: the case of China *Environ. Res. Lett.* **15** 064027
- [38] Mohr C *et al* 2012 Identification and quantification of organic aerosol from cooking and other sources in Barcelona using aerosol mass spectrometer data *Atmos. Chem. Phys.* **12** 1649–65
- [39] Decarlo P F *et al* 2006 Field-deployable, high-resolution, time-of-flight aerosol mass spectrometer *Anal. Chem.* **78** 8281–9
- [40] Sueper D, Allan J D, Dunlea E, Crosier J, Kimmel J R, DeCarlo P F, Aiken A C and Jimenez J L 2007 A Community Software for Quality Control and Analysis of Data from the Aerodyne Time-of-Flight Aerosol Mass Spectrometers (ToF-AMS) *Tech. rep.* Reno, NV <http://cires1.colorado.edu/events/rendezvous/2008/posters/sueper.html>
- [41] Mohr C, Huffman J A, Cubison M J, Aiken A C, Docherty K S, Kimmel J R, Ulbrich I M, Hannigan M and Jimenez J L 2009 Characterization of primary organic aerosol emissions from meat cooking, trash burning, and motor vehicles with high-resolution aerosol mass spectrometry and comparison with ambient and chamber observations *Environ. Sci. Technol.* **43** 2443–9
- [42] Jimenez J L *et al* 2009 Evolution of organic aerosols in the atmosphere *Science* **326** 1525–9
- [43] Alameda County Department of Environmental Health (www.gis.acgov.org/DEH/InspectionResults)
- [44] City of Berkeley Data Services (https://www.cityofberkeley.info/404.aspx?aspxerrorpath=/Health_Human_Services/Environmental_Health/Online_Food_Facility_Inspection_Results.aspx)
- [45] Allegheny County Restaurant/Food Facility Inspections (<https://data.wprdc.org/dataset/allegheny-county-restaurant-food-facility-inspection-violations>)
- [46] Yelp (<https://www.yelp.com/>)
- [47] Alameda county data sharing initiative (<https://data.acgov.org/>)
- [48] Allegheny County GIS Open Data (<https://data.acgov.org/Geospatial-Data/Alameda-County-Street-Centerlines/wjre-3857>)
- [49] US Census Bureau: American Fact Finder (<https://factfinder.census.gov/faces/nav/jsf/pages/index.xhtml>)
- [50] Messier K P *et al* 2018 Mapping air pollution with google street view cars: efficient approaches with mobile monitoring and land use regression *Environ. Sci. Technol.* **52** 12563–72
- [51] Zhang Q, Gangupomu R H, Ramirez D and Zhu Y 2010 Measurement of ultrafine particles and other air pollutants emitted by cooking activities *Int. J. Environ. Res. Public Health* **7** 1744–59
- [52] Vert C, Meliefste K and Hoek G 2016 Outdoor ultrafine particle concentrations in front of fast food restaurants *J. Expo. Sci. Environ. Epidemiol.* **26** 35–41
- [53] Katragadda H R, Fullana A, Sidhu S and Carbonell-Barrachina A A 2010 Emissions of volatile aldehydes from heated cooking oils *Food Chem.* **120** 59–65
- [54] Moumtaz S, Percival B C, Parmar D, Grootveld K L, Jansson P and Grootveld M 2019 Toxic aldehyde generation in and food uptake from culinary oils during frying practices: peroxidative resistance of a monounsaturate-rich algae oil *Sci. Rep.* **9** 1–21
- [55] Karner A A, Eisinger D S and Niemeier D A 2010 Near-roadway air quality: Synthesizing the findings from real-world data *Environ. Sci. Technol.* **44** 5334–44
- [56] Saha P K, Khlystov A, Snyder M G and Grieshop A P 2018 Characterization of air pollutant concentrations, fleet emission factors, and dispersion near a North Carolina interstate freeway across two seasons *Atmos. Environ.* **177** 143–53
- [57] Preble C V, Cados T E, Harley R A and Kirchstetter T W 2018 In-use performance and durability of particle filters on heavy-duty diesel trucks *Environ. Sci. Technol.* **52** 11913–21
- [58] Von Der Weiden-Reinmüller S L, Drewnick F, Zhang Q J, Freutel F, Beekmann M and Borrmann S 2014 Megacity emission plume characteristics in summer and winter investigated by mobile aerosol and trace gas measurements: The Paris metropolitan area *Atmos. Chem. Phys.* **14** 12931–50
- [59] Elser M *et al* 2016 Urban increments of gaseous and aerosol pollutants and their sources using mobile aerosol mass spectrometry measurements *Atmos. Chem. Phys.* **16** 7117–34